MATHEMATICAL BIOSCIENCES
AND ENGINEERING
Volume **4**, Number **1**, January **2007**

http://www.mbejournal.org/

pp. **15–28**

FOREST DEFOLIATION SCENARIOS

Glenn Ledder

Department of Mathematics, University of Nebraska-Lincoln
Lincoln, NE 68588-0130

Abstract. We consider the mathematical model originally created by Ludwig, Jones, and Holling to model the infestation of spruce forests in New Brunswick by the spruce budworm. With biologically plausible parameter values, the dimensionless version of the model contains small parameters derived from the time scales of the state variables and smaller parameters derived from the relative importance of different population change mechanisms. The small time-scale parameters introduce a singular perturbation structure to solutions, with one variable changing on a slow time scale and two changing on a fast time scale. The smaller process-scale parameters allow for the existence of equilibria at vastly different orders of magnitude. These changes in scale of the state variables result in fast dynamics not associated with the time scales. For any given set of parameters, the observed dynamics is a mixture of time-scale effects with process-scale effects. We identify and analyze the different scenarios that can occur and indicate the relevant regions in the parameter space corresponding to each.

1. **Introduction.** The spruce budworm model of Ludwig, Jones, and Holling [8] has become a classic example of nonlinear population dynamics because of the existence of a stable periodic orbit that shows good agreement with data obtained from a spruce forest in New Brunswick. Portions of the model have appeared in several textbooks [7, 6], and the full model has appeared in at least two [4, 1]. None of these treatments is complete in the sense of correctly identifying all of the model behaviors that can be obtained over a wide range of parameter values. In this paper, we describe the various scenarios that can arise, detail the specific behavior of each, and indicate the circumstances in which each scenario can arise. The model is seen to exhibit a rich variety of behaviors despite being a caricature rather than a complete description of forest dynamics.

The standard approach in the analysis of dynamical systems with variables that change at very different rates is to use singular perturbation to identify slow periods, during which the fast variables are in quasi-equilibrium, and fast periods, during which the slow variables are roughly constant and the fast variables approach a new quasi-stable equilibrium [11]. The singular perturbation method can be advantageously combined with geometric analysis to yield additional insights into the complex behavior of dynamical systems [3, 10, 9, 2].

A complete treatment of the LJH model requires a more sophisticated use of dominant balance arguments and quasi-equilibria than the classic singular perturbation scheme because the various stable quasi-equilibria are of very different orders

2000 *Mathematics Subject Classification.* 92D40, 34E15.
Key words and phrases. singular perturbation, defoliation, spruce budworm.

of magnitude and because those orders of magnitude have a dramatic effect on the rates of change. This situation results from two factors that are not often present in singular dynamical system models: (1) the presence of terms on the right-hand sides of the equations that contain parameters significantly smaller than the time-scale parameters, and (2) rates that can become large when dynamic variables are small. It is therefore necessary to delineate several regimes, each with its own scaling of the dependent variables, with the singular perturbation method applied separately to each regime.

In the development that follows, we attempt to provide a careful outline of the use of dominant balance and singular perturbation arguments to analyze models that feature complex dynamics with a variety of possible scenarios delineated by various ranges of parameter values. We also emphasize the connections between the different scenarios and the biological processes in the model, with the goal of yielding further insight into the question of what biological differences between specific ecological systems lead to the different observed outcomes.

2. **The forest defoliation model.** The forest defoliation model of Ludwig, Jones, and Holling [8] (see Fowler [4] for a derivation and scaling of the model) is a system of three nonlinear ordinary differential equations:

$$\epsilon_1 \frac{dB}{dt} = B\left[1 - \frac{B}{S}\left(\frac{\delta^2 + E^2}{E^2}\right)\right] - \frac{\lambda B^2}{\nu^2 S^2 + B^2}, \tag{1}$$

$$\epsilon_2 \frac{dE}{dt} = E(1-E) - \frac{\gamma B}{S}\left(\frac{E^2}{\delta^2 + E^2}\right), \tag{2}$$

$$\frac{dS}{dt} = S\left(1 - \frac{S}{E}\right). \tag{3}$$

Here B is the population density of consumers (spruce budworms in the original) per unit land area, E is a measure of the average tree health, roughly equivalent to the density of leaves per unit surface, and S is a measure of the forest density, roughly equivalent to the amount of tree surface area per unit land area. The factors ϵ_1 and ϵ_2 are the ratios of the characteristic times of the consumers and the tree health, respectively, to that of the forest density. These ratios should be small and comparable, and they are usually taken as 1/15 and 1/9, respectively. Each of the dynamic variables is governed by a modified version of the logistic equation. The equation (3) for the tree density differs from the logistic equation only in that the environmental capacity is taken to be the tree health rather than a fixed parameter. The capacity for the tree health is unity, and the capacity for the consumer population is the tree density S reduced by the factor $E^2/(\delta^2 + E^2)$ when the tree health is particularly low. The parameter δ represents the level of tree health for which consumer capacity per tree surface area is half its normal value. The additional term in the tree health equation represents the damage done to the trees by the consumers; this damage is assumed to be proportional to the density of consumers per unit tree surface, again reduced by the factor $E^2/(\delta^2+E^2)$ when the tree health is particularly low. The parameter γ represents the maximum damage rate relative to the tree health time scale. The additional term in the consumer equation represents predation (by birds in the original). The predators are assumed to have a variety of food sources. Since they do not rely on the population of our particular consumer, we may safely assume their population to be independent of B. Thus, the predators are represented by a maximum kill rate λ and a functional

response indicating the density dependence of that kill rate. The sigmoidal Holling type 3 [5] functional response is preferable when predators have alternative food sources. The parameter ν measures the density of consumers per tree surface area at which predation is reduced by half. The density of consumers per tree surface area (B/S) is more meaningful in this context than the density of consumers per land area (B) because the density per tree area is what determines the ease with which the predators can spot and kill their prey. For this reason, we will sometimes find it useful to plot B/S rather than B.

2.1. **An interesting example.** Imagine a four-dimensional space of the parameters γ, δ, λ, and ν. Hypersurfaces in this space mark the boundaries between different possible behaviors of the system. With focused hindsight, it is possible to choose a set of parameter values that lies in the region with the most interesting behavior, but near all of these hypersurfaces. Here, we choose the parameter set

$$\gamma = 0.3, \quad \epsilon_1 = \frac{1}{15}, \quad \epsilon_2 = \frac{1}{9}, \quad \delta = 0.03, \quad \lambda = 0.003, \quad \nu = 0.00167. \tag{4}$$

as a specific example.[1] In this set of values, γ is the only parameter that is not small. The parameters λ and ν are significantly smaller than the time scale parameters; hence, the system admits of both singular perturbation with small parameters ϵ_1 and ϵ_2 and regular perturbation with smaller parameters ν, λ, and δ. We want the model to represent defoliation scenarios, but we don't want to overly restrict the possible behaviors of the model. In the subsequent analysis, we assume

$$\lambda, \nu \ll \epsilon_1, \epsilon_2 \ll 1, \qquad \frac{\epsilon_1}{\epsilon_2} = \mathcal{O}(1), \quad \frac{\lambda}{\nu} = \mathcal{O}(1). \tag{5}$$

We leave open for now the issue of whether to take δ to be comparable to ϵ_1, comparable to λ, or of an order between the two.

Figures 1 and 2 illustrate the results of a computer simulation using our example. We see a stable periodic solution (period ≈ 13) that exhibits two slow stages characterized by approximately fixed values of E, separated by stages in which E is changing rapidly. The vertical lines in the time series graphs indicate the approximate boundaries of several different regimes, each distinguished by the orders of magnitude of the dependent variables and the time scale on which significant changes occur. Regime IV is very brief, with its location indicated by the vertical line separating Regimes III and V. Figure 2b shows a cross-section of the B nullcline surface on a plane parallel to the SB-coordinate plane. This cross-section is correct when $E \gg \delta$, but not when $E = \mathcal{O}(\delta)$ or $E \ll \delta$. Note also that the portion of the nullcline surface having $B \ll 1$ extends only to the value $S = \sigma < 1$, where $\sigma = \lambda/(2\nu)$. Similarly, the quasi-equilibrium curve in Figure 2a extends only to $S = \sigma$.

Our example serves as an excellent backdrop for the explanation of the different regimes. Once we understand the example, other scenarios can be easily explained by comparison.

[1]The values for the time-scale parameters are those reported in the literature, while the other parameters have been chosen for mathematical interest. However, none of the parameters differs from its typical value by as much as a factor of three (Fowler [4] gives $\gamma = 0.7$, $\delta = 0.02$, $\lambda = 0.004$, and $\nu = 0.003$), so conceivably these parameter values could apply to some forest system similar to the spruce budworm forest used to obtain the parameter estimates.

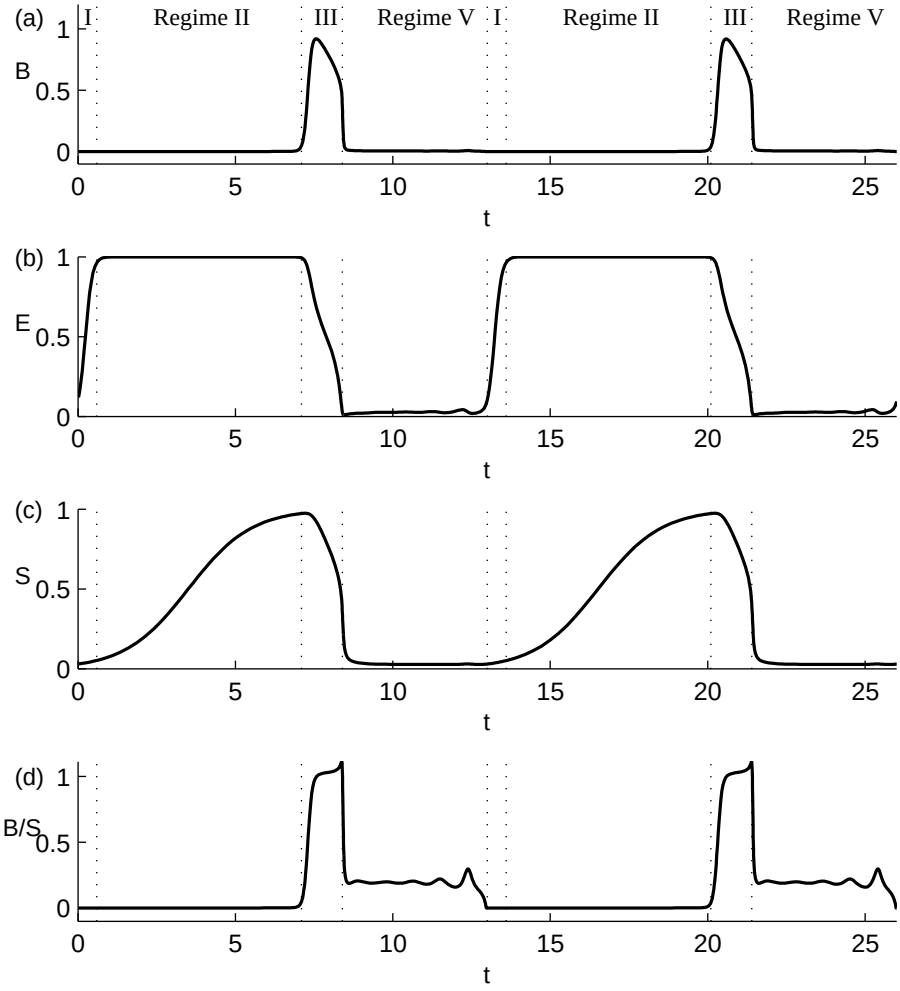

FIGURE 1. Time series for the example, with approximate delineation of several distinct regimes.

3. **Analysis of the model.** A considerable insight into the possible behaviors of the model can be gleaned from a careful examination of the equations, prior to any mathematical analysis. Note that dB/dt is positive as $B \to 0$ and negative as $B \to S$. From this and similar considerations, we see that stable equilibria must have $0 < B < S = E < 1$. Predation will occur at a constant maximum rate whenever the consumer-to-surface ratio B/S is much greater than ν; however, this predation can limit the consumer population only when the consumer population is $\mathcal{O}(\lambda)$ or smaller.

Based on a quick inspection of the differential equations, $\mathcal{O}(1)$ changes in B and E would seem to occur in time intervals of $\mathcal{O}(\epsilon_i)$. However, the changes will not be so fast when the solution lies near the curve marking the intersection of the B and E nullcline surfaces. At such points, the right sides of equations (1) and (2) will be small, and changes will occur at a slower rate. It is as if the BE subsystem were at equilibrium, except that the value of S is slowly changing rather than

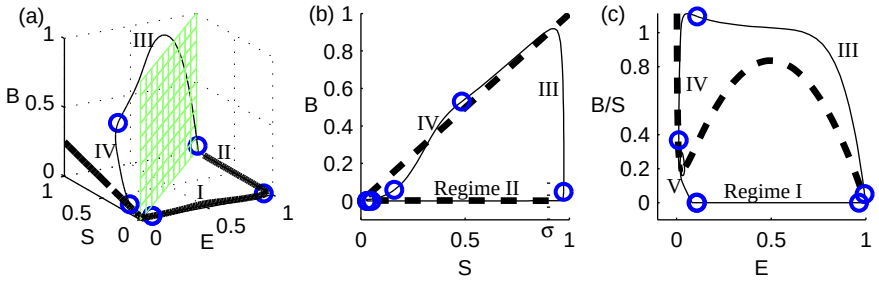

FIGURE 2. Phase portrait for the example. The circles mark the approximate boundaries between regimes. The heavy curves mark the BE quasi-equilibrium curve, the B nullcline surface (except where E is small), and the E nullcline surface, respectively. The plane in (a) is the S nullcline surface.

constant; hence, it makes sense to use the term "quasi-equilibrium" to describe equilibria in the BE subsystem. When the system is at quasi-equilibrium, the observed dynamics is driven by equation (3), and is therefore said to be "slow." The values of B and E change via the movement of the solution along the quasi-equilibrium curve. If the parameter values are such that the solution can follow the quasi-equilibrium curve all the way to the S nullcline surface, the system will evolve to a stable equilibrium. Regimes II and V in Figure 1 are typical examples of slow dynamics; in both cases, the solution curve follows the quasi-equilibrium curve for a while, but it cannot follow the quasi-equilibrium curve all the way to the S nullcline surface. Eventually, S increases or decreases to a point where the solution must leave the quasi-equilibrium curve, and the dynamics ceases to be slow.

Suppose the system is at a state that is not close to the quasi-equilibrium curve. Then at least one of B and E will exhibit $\mathcal{O}(1)$ changes in time intervals of $\mathcal{O}(\epsilon_i)$, ending when quasi-equilibrium is restored, either because the solution is near the quasi-equilibrium curve or because either B or E has become small. During these short time intervals, changes in S are relatively small. The observed dynamics in these intervals is said to be "fast." Regimes I and III in Figure 1 are typical examples of fast dynamics.

Regime IV is somewhat different from the standard fast regimes characteristic of singularly perturbed dynamical systems because the "slow" variable S exhibits fast changes. Why does this occur? In typical singularly-perturbed dynamical systems, the dependent variables are sometimes small, and normally this can slow the dynamics, as we see in Regime V. What is unusual about the forest defoliation model is that small variable values can make the dynamics faster. The factor E in the denominators of the B and S equations, rather than the small parameters ϵ_i, is responsible for the fast dynamics of Regime IV. Rapid decreases in S occur whenever E is small relative to S. The rate of these changes depends on the correct rescaling of E for that regime. In biological terms, the environmental capacity changes by an order of magnitude comparable to or larger than the ratio of the time scales.

These observations serve to explain the qualitative features of the complex limit cycle illustrated in Figures 1 and 2. However, it is essential to note that we could not have obtained a set of parameter values to produce this complex limit cycle without

having already identified, through asymptotic analysis, the various scenarios that the model can produce, which include several simpler scenarios as well as the cycle we have been examining. Simulations with different sets of parameter values can be used to obtain a sampling of possible behaviors of a dynamical system, but only analysis can guarantee that all possible behaviors have been found.

In the asymptotic analysis that follows, we want to tease out the proper orderings for the three dynamic variables. There are two basic principles that must be followed. First, we may make any initial assumptions about possible orderings as long as we are careful not to omit any possible cases. We will sometimes be explicit about ordering assumptions from the outset; at other times, we will benefit by postponing such explicit assumptions. Second, we must only discard terms that are clearly dominated by other terms, given the postponement of explicit ordering assumptions.

3.1. **Regimes I and II.** We begin by looking at the model under the assumptions $E, S = \mathcal{O}(1)$ and $B \ll S$, which appear to be appropriate for Regime II. As immediate consequences of these assumptions, we have

$$\frac{B}{S}\left(\frac{\delta^2 + E^2}{E^2}\right) \ll 1, \qquad \frac{\gamma B}{S}\left(\frac{E^2}{\delta^2 + E^2}\right) \ll E(1-E);$$

we may therefore simplify the BE subsystem to

$$\epsilon_1 \frac{dB}{dt} = B - \frac{\lambda B^2}{\nu^2 S^2 + B^2}, \tag{6}$$

$$\epsilon_2 \frac{dE}{dt} = E(1-E). \tag{7}$$

This system is decoupled, with $E = 1$ a stable equilibrium for the second equation. We now assume $B = \mathcal{O}(\lambda)$ to balance the growth and predation terms in equation (6) and admit a possible quasi-equilibrium solution. The substitution

$$b = \lambda^{-1} B$$

yields the rescaled equation

$$\epsilon_1 \frac{db}{dt} = b\left(1 - \frac{b}{(\nu S/\lambda)^2 + b^2}\right). \tag{8}$$

Given S as a fixed parameter (a reasonable assumption for times of $\mathcal{O}(\epsilon_1)$), equation (8) has the equilibrium solutions

$$b = \frac{1 \pm \sqrt{1 - (2\nu S/\lambda)^2}}{2},$$

provided $S < \lambda/(2\nu)$. The smaller of these solutions is asymptotically stable, so these scalings yield a stable quasi-equilibrium solution

$$B \sim \frac{\lambda}{2}\left(1 - \sqrt{1 - \left(\frac{S}{\sigma}\right)^2}\right), \quad E \sim 1, \quad S < \sigma \equiv \frac{\lambda}{2\nu}, \tag{9}$$

which is what we see in Regime II.

The initial conditions used in the simulation do not satisfy the quasi-equilibrium equations because of the small starting value of E. Thus, Regime II is preceded by a fast regime (Regime I), in which E changes on the fast scale to the stable quasi-equilibrium (9). Then (Regime II) S increases on the slow time scale toward $S = 1$, B increases with S according to (9), and E is fixed at 1. If $\lambda < 2\nu$, the slow

phase ends when S reaches the critical value $\lambda/(2\nu)$, at which point equation (8) no longer has an equilibrium solution. In our example, this occurs at $t \approx 7$, and Regime II ends as B increases to $\mathcal{O}(1)$. Figure 3 shows the time series curves and the b versus S curve for Regimes I and II for the example. The Sb plane shows why the solution must leave the quasi-equilibrium curve: S must increase because $S < E$, yet the quasi-equilibrium curve reaches a maximum at $S = \sigma < 1$. If the quasi-equilibrium curve were extended farther to the right, it would be possible for the solution curve to follow it all the way to $S = 1$, achieving an equilibrium state with trees at full health.

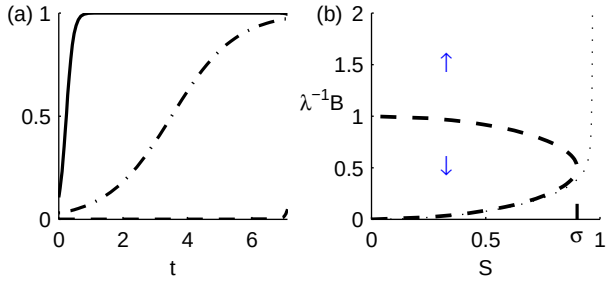

FIGURE 3. Regimes I and II (a: dash=B, solid=E, dash-dot=S; b: dash=B-nullcline surface, dot=solution curve).

3.2. **Regime III.** Regime II ends with $\lambda^{-1}B \to \infty$, so we next consider the case of $E, S, B = \mathcal{O}(1)$. Here, the BE subsystem is given by

$$\epsilon_1 \frac{dB}{dt} = B\left(1 - \frac{B}{S}\right), \tag{10}$$

$$\epsilon_2 \frac{dE}{dt} = E(1-E) - \frac{\gamma B}{S}. \tag{11}$$

This system is decoupled, with $B = S$ a stable quasi-equilibrium for the first equation. The second equation then has the equilibria

$$E = \frac{1 \pm \sqrt{1-4\gamma}}{2},$$

provided $\gamma < \frac{1}{4}$. The larger of these two solutions is asymptotically stable, so Regime II yields a stable equilibrium solution

$$B, E, S \sim \frac{1}{2}(1 + \sqrt{1-4\gamma}), \qquad \gamma < \frac{1}{4}. \tag{12}$$

In Regime III, B approaches S on the fast time scale, while E decreases rapidly, as illustrated in Figure 4. If $\gamma > \frac{1}{4}$, as in the example, the B and E nullcline surfaces do not intersect; consequently, there is no quasi-equilibrium solution and only fast dynamics occur. Decreasing γ raises the E nullcline surface. If $\gamma < \frac{1}{4}$, the surface is high enough that it intersects the B nullcline surface, forming a quasi-equilibrium curve that is not present in our example. This curve would appear in Figure 4c as the rightmost of the two points of intersection. In this case, the solution will move on the fast time scale to the quasi-equilibrium curve and then follow it, on the slow time scale, to the stable equilibrium point (12).

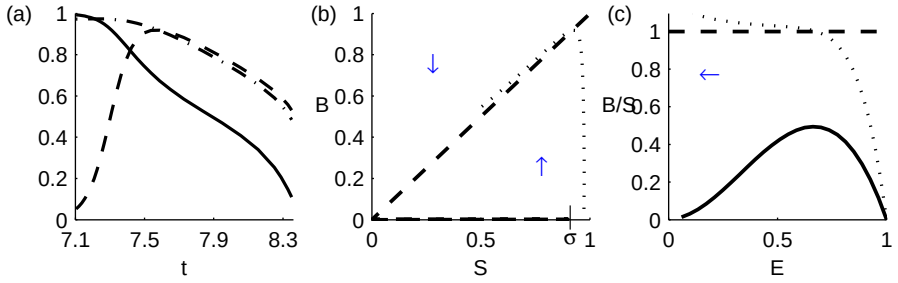

FIGURE 4. Regime III (a: dash=B, solid=E, dash-dot=S; b, c: dash=B-nullcline surface, solid=E-nullcline surface, dot=solution curve).

3.3. **Regime IV.** We have now completely analyzed the regimes in which S and E are $\mathcal{O}(1)$. We turn now to $E = \mathcal{O}(\delta)$, which is the ordering in which the factor $E^2/(\delta^2 + E^2)$ will be retained. With the substitution

$$\bar{E} = \delta^{-1} E,$$

the full system becomes

$$\epsilon_1 \frac{dB}{dt} = B\left[1 - \frac{B}{S}\left(\frac{1+\bar{E}^2}{\bar{E}^2}\right)\right] - \frac{\lambda B^2}{\nu^2 S^2 + B^2}, \tag{13}$$

$$\epsilon_2 \frac{d\bar{E}}{dt} = \bar{E} - \frac{\gamma B}{\delta S}\left(\frac{\bar{E}^2}{1+\bar{E}^2}\right), \tag{14}$$

$$\frac{dS}{dt} = S - \frac{S^2}{\delta \bar{E}}. \tag{15}$$

Given $E = \mathcal{O}(\delta)$, we see from equation 15 that an equilibrium solution can only occur with $S = \mathcal{O}(\delta)$. Similarly, examination of equation 14 shows that $B = \mathcal{O}(\delta^2)$ is the only ordering that can yield an equilibrium solution in the full system or the BE subsystem. However, these assumptions result in the approximation

$$\epsilon_1 \frac{dB}{dt} = B - \lambda,$$

which admits no stable equilibria. Thus, Regime IV is a fast regime governed by equations 13–15, with some appropriate ordering for B and S. Clearly $S = \mathcal{O}(1)$, because S is a slow variable and was $\mathcal{O}(1)$ in the previous regime. There is no loss of generality in assuming $B = \mathcal{O}(1)$, which is consistent with the earlier observation that the solution is on the B nullcline surface at the end of Regime III. With these scalings, the leading order B and S equations are

$$\epsilon_1 \frac{dB}{dt} = B\left[1 - \frac{B}{S}\left(\frac{1+\bar{E}^2}{\bar{E}^2}\right)\right] \tag{16}$$

$$\frac{dS}{dt} = -\frac{S^2}{\delta \bar{E}}. \tag{17}$$

The rescaling of E makes S a fast variable that should undergo $\mathcal{O}(1)$ changes in time intervals of $\mathcal{O}(\delta)$. This makes the dynamics in Regime IV faster than the "fast" dynamics of Regimes I and III. Figure 5 illustrates the details of the dynamics of Regime IV.

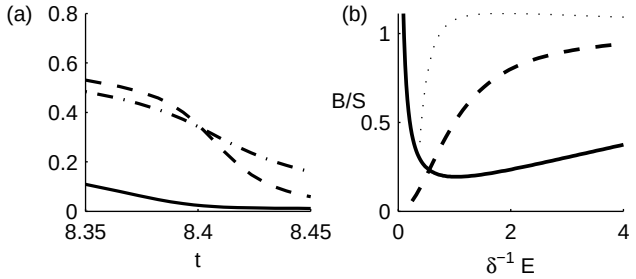

FIGURE 5. Regime IV (a: dash=B, solid=E, dash-dot=S; b: dash=B-nullcline surface, solid=E-nullcline surface, dot=solution curve).

3.4. **Regime V.** We have considered all possible regimes with $E \gg \delta$ and with $E = \mathcal{O}(\delta)$. It remains to consider the possibility of a slow regime with $\mathcal{O}(S) = \mathcal{O}(E) \ll \delta$. With these scalings, the BE subsystem becomes

$$\epsilon_1 \frac{dB}{dt} = B\left(1 - \frac{\delta^2 B}{SE^2}\right) - \frac{\lambda B^2}{\nu^2 S^2 + B^2}, \tag{18}$$

$$\epsilon_2 \frac{dE}{dt} = E\left(1 - \frac{\gamma B}{\delta^2}\frac{E}{S}\right). \tag{19}$$

A nontrivial equilibrium for equation 19 requires $B = \mathcal{O}(\delta^2)$. Then $\nu S \ll \nu\delta < \delta^2$, so $\nu S \ll B$ and the B equation simplifies further to

$$\epsilon_1 \frac{dB}{dt} = B\left(1 - \frac{\delta^2 B}{SE^2} - \frac{\lambda}{B}\right). \tag{20}$$

We must now have $SE^2 = \mathcal{O}(\delta^2 B)$, so $S, E = \mathcal{O}(\delta^{4/3})$. Hence, either $\lambda = \mathcal{O}(\delta^2)$ or $\lambda \ll \delta^2$; we assume the former to retain more of the dynamics. Note that this scaling is not substantially different from $E = \mathcal{O}(\delta)$. One consequence of this is that we can arbitrarily decide to continue to plot $\delta^{-1}E$ as the tree health variable, rather than the more complicated $\delta^{-4/3}E$. Another consequence is that the simplification $\delta^2 + E^2 \sim \delta^2$ used in this scaling results in a perturbation expansion in which the first correction term is $\mathcal{O}([\delta/\gamma]^{2/3})$ relative to the leading order solution. Despite the relatively large size of this correction term, the asymptotic results are borne out by numerical simulations.

To simplify the subsequent calculations in this regime, we make the substitutions

$$E = \frac{\delta^{4/3}}{\gamma^{1/3}}e, \qquad S = \frac{\gamma^{2/3}\lambda}{\delta^{2/3}}s, \qquad B = \lambda b, \qquad \eta = \frac{\gamma\lambda}{\delta^2}.$$

In addition to correctly scaling the variables, these substitutions yield a system in which the quasi-equilibrium equations contain no parameters other than s:

$$\epsilon_1 \frac{db}{dt} = b\left(1 - \frac{b}{se^2} - \frac{1}{b}\right), \tag{21}$$

$$\epsilon_2 \frac{de}{dt} = e\left(1 - \frac{be}{s}\right), \tag{22}$$

$$\frac{ds}{dt} = s\left(1 - \frac{\eta s}{e}\right). \tag{23}$$

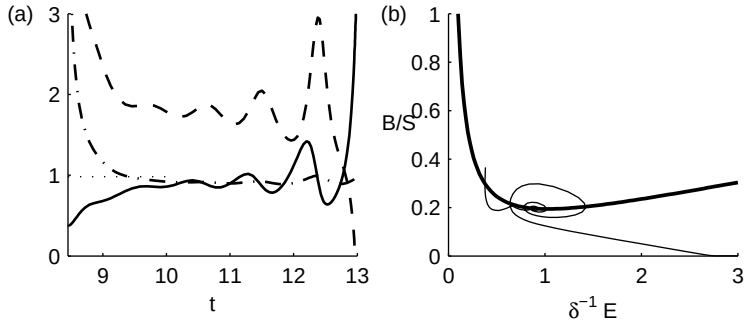

FIGURE 6. Regime V (a: dash=b, solid=$\delta^{-1}E$, dash-dot=$\delta^{-1}S$, dot=$\delta^{-1}S_{cr}$; b: thick=E-nullcline surface, thin=solution curve).

Analysis of the BE subsystem yields the result that there are quasi-equilibrium solutions $b = b^*$, $e = s/b^*$, where b^* is a solution of the equation

$$\frac{b^4}{b-1} = s^3.$$

This equation has two solutions whenever

$$s > \frac{2^{8/3}}{3} \equiv s_{cr},$$

the larger of the two being stable provided either

$$\epsilon_2 < 2\epsilon_1 \quad \text{or} \quad b^* > \frac{2\epsilon_2}{\epsilon_1 + \epsilon_2}.$$

For our study, the first condition is always met; hence, this scaling does have a stable quasi-equilibrium solution. If this solution is achieved, the result could be either progression to the full equilibrium solution, given by

$$b = \eta^{-1}, \qquad e = (1-\eta)^{-1/3}, \qquad s = be, \tag{24}$$

which is asymptotically stable if

$$\eta < \min\left(\frac{3}{4}, \frac{\epsilon_1 + \epsilon_2}{2\epsilon_1}\right),$$

or progression to a point where $s < s_{cr}$. The latter occurs in our example, as illustrated in Figure 6. Points where the trajectory is horizontal indicate approximate points on the B nullcline surface. When S drops below the minimum value for a quasi-stable equilibrium, the solution oscillates with growing amplitude until $b < 1$. At this point, the consumer population drops drastically because the gain from growth is no longer sufficient to offset the loss from predation. This drastic reduction can be seen at the boundary between Regime V and the subsequent Regime I.

TABLE 1. Properties of the five regimes in the example. ($k = \min(0.75, 0.5[\epsilon_1 + \epsilon_2]/\epsilon_1)$, NCS=nullcline surface, QEC=quasi-equilibrium curve)

	E	S	B/S	B	time scale	location	stable equilibrium
I	$\mathcal{O}(1)$	$\ll 1$	$\ll 1$	$\ll \lambda$	$\mathcal{O}(\epsilon_2)$	B NCS	never
II	~ 1	$\mathcal{O}(1)$	$\mathcal{O}(\lambda)$	$\mathcal{O}(\lambda)$	$\mathcal{O}(1)$	QEC	if $\lambda > 2\nu$
III	$\mathcal{O}(1)$	$\mathcal{O}(1)$	$\mathcal{O}(1)$	$\mathcal{O}(1)$	$\mathcal{O}(\epsilon_2)$	B NCS	if $\gamma < 1/4$
IV	$\mathcal{O}(\delta)$	$\mathcal{O}(1)$	$\mathcal{O}(1)$	$\mathcal{O}(1)$	$\mathcal{O}(\delta)$	E NCS	never
V	$\mathcal{O}(\delta^{4/3})$	$\mathcal{O}(\delta^{4/3})$	$\mathcal{O}(\delta^{2/3})$	$\mathcal{O}(\lambda)$	$\mathcal{O}(1)$	QEC	if $\gamma\lambda < k\delta^2$

4. **Results and discussion.** Table 1 summarizes the properties of the five regimes, including the orderings of the dynamic variables, the time scale with the parameter values in the example, the location of the solution curve relative to the nullcline surfaces of the fast variables, and the possible existence of stable equilibria for other sets of parameter values.

Suppose we have the initial data $B = B_0 \approx \lambda$, $E = 1$, $S = 1$, corresponding to a small but significant initial consumer population in a forest not previously exposed to the consumers. Based on the information in the last column of Table 1, we can delineate four basic scenarios:

1. An endemic infestation scenario, consisting of a stable equilibrium in Regime III, will occur if $\gamma < 1/4$.
2. An ecological disaster scenario, consisting of a stable equilibrium in Regime V, will occur if $\gamma > 1/4$ and $\gamma\lambda < k\delta^2$, where $k = \min(0.75, 0.5[\epsilon_1 + \epsilon_2]/\epsilon_1)$.
3. A temporary defoliation scenario, consisting of a stable equilibrium in Regime II, will occur if $\gamma > 1/4$, $\gamma\lambda > k\delta^2$, and $\lambda > 2\nu$.
4. A limit cycle with a long period of depression (Regime V), as seen in the first example, will occur if none of the conditions leading to stable equilibria exist.

Two additional scenarios can occur if we relax some of the restrictions imposed on the above.

5. A nonevent scenario, consisting of a stable equilibrium in Regime II without moving through the cycle once, can occur if the initial consumer level is below the value given by the larger of the equilibrium solutions of equation 8. This scenario is of minimal interest, as there would be no observations to call attention to an outbreak that is contained without affecting tree health.
6. A limit cycle with a short period of depression can occur if none of the other equilibria are indicated and $\delta^2 \ll \lambda$.

TABLE 2. Parameter values for scenarios 1–6

Scenario	γ	λ	ν	δ	$B0$
1	0.24	0.0030	0.00167	0.03	0.003
2	0.30	0.0021	0.00167	0.03	0.003
3	0.30	0.0036	0.00167	0.03	0.003
4	0.30	0.0030	0.00167	0.03	0.003
5	0.30	0.0036	0.00167	0.03	0.002
6	0.70	0.0040	0.00300	0.02	0.003

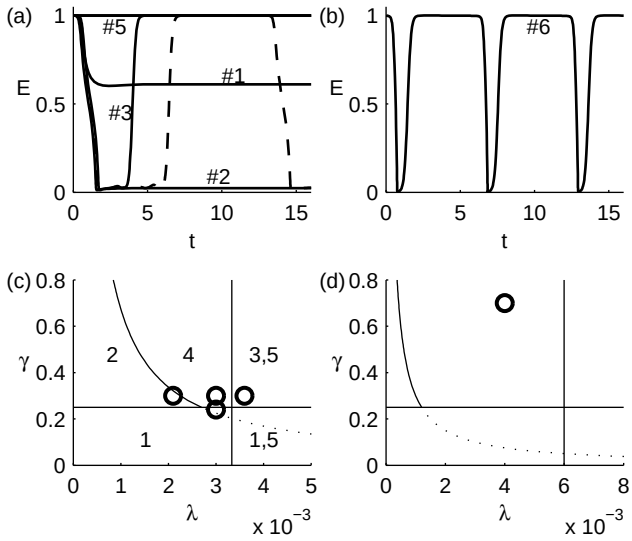

FIGURE 7. Tree health and bifurcation plot for scenarios 1–6. The dashed curve in (a) is scenario 4. The numbers in (c) indicate the scenarios corresponding to each region in the parameter space.

These scenarios are illustrated in Figure 7, using the parameter values indicated in Table 2. The parameters in scenario 6 are those estimated by Ludwig, Jones, and Holling [8] and/or Fowler [4]. In each case, we illustrate the scenario using a plot of tree health. Scenario 5 uses the same parameters as scenario 3, except that the initial consumer population is smaller. Scenario 4 is the complex limit cycle of our example. We consider each of these scenarios in turn.

- **endemic infestation**
  The lower value of γ means that the consumers are not quite as damaging to the trees as in the standard example. The quasi-stable equilibrium of Regime III exists in this case. It is quickly achieved and evolves to the stable equilibrium solution with all variables $\mathcal{O}(1)$. The cycle is broken because the tree health does not fall far enough to ruin the consumer habitat.
- **ecological disaster**
  With a small decrease in λ, the solution is nearly the same as the standard example through the first four regimes. In Regime V, however, the solution reaches the stable equilibrium in which $E = \mathcal{O}(\delta^{4/3})$. Here, the maximum predation rate is not sufficient to cause the consumer population to crash, so the tree health is never able to recover. Scenario 2 is observed when an invasive insect pest causes the local extinction of the affected tree species. Note that the equilibrium state achieved in scenario 2 is also stable when the parameters lie in regions marked "1" in Figure 7c and below the dotted curve; however, this equilibrium state is not achieved in these regions with realistic initial conditions.
- **temporary defoliation or nonevent**
  A slight increase in λ has the effect of making the crash in the consumer population happen earlier, leading to an earlier recovery of tree health. Moreover, if the maximum predation rate is large enough, then the tree surface area

needed to enable the explosive population growth of the consumer (Regime III) is larger than what can be achieved at maximum tree health. As a result, the stable equilibrium solution of Regime II exists and can be achieved. In scenario 3, the initial consumer density is above the equilibrium curve in Figure 3b. This means that the system goes through one full cycle before eventually approaching the stable equilibrium. With a more modest initial consumer density, as in scenario 5, the system evolves immediately to the stable equilibrium solution without going through one defoliation cycle. In this case, there is no observable change from the initial maximum tree health.

- **limit cycle with long period of depression**
  Scenario 4 differs from our standard example only in the initial conditions, which are similar to the solution values that we see near the end of Regime II. The system approaches the stable periodic orbit quickly. The tree health remains high until the end of Regime II, which occurs very quickly with the given set of initial conditions. The tree health falls precipitously in Regime III when the consumer population is briefly $\mathcal{O}(1)$, remains low in Regime IV during the rapid decline of the consumer population, and oscillates at a low value during Regime V. Regime I begins at about time 6, with the tree health rapidly rising up to its normal value. The cycle of defoliation begins again at about time 13.
- **limit cycle with short period of depression**
  The significant difference between scenario 6 and scenario 4 is in the location of the hypersurface that separates scenarios 2 and 4. The parameter set reported for the spruce budworm forest has a noticeably smaller semi-saturation level for the effect of tree health on consumption. With $\gamma\lambda \gg \delta^2$, Regime V has no quasi-equilibrium. It is therefore very short-lived, with the drastic reduction in consumer population occurring immediately, rather than over time as in Figure 6. The result is that Regimes IV, V, and I merge into a single fast regime marked by a rapid recovery of tree health following the very quick decrease in consumers. In practice, we would expect this scenario to be more likely than our primary example, which was chosen for its mathematical interest rather than its accuracy in describing real systems. When the parameters are within the space in which the tree health is low for a long period, as in our primary example, we might anticipate that other factors, such as competition among tree species, would intervene to drive the affected tree species to local extinction, as in scenario 2.

5. **Conclusions.** A complete explanation of the dynamics of the LJH forest defoliation model requires consideration of the effects of small parameters on the right-hand sides of the dynamic equations as well as small parameters that represent the ratios of time scales. Small parameters appear on the right-hand side in any model in which the relative importance of the different contributing processes depends strongly on the magnitudes of the dependent variables. In the forest defoliation model, for example, predation can be a key process in the limitation of the consumer population; however, predation is insufficient to affect the consumer population unless that population is already much smaller than at breakout levels. Normally, predation at low levels plays only a minimal role in limiting population size. In the LJH model, however, the capacity of the environment to support the consumer population is reduced by the success of those consumers in exploiting

that environment. Eventually, the reduced environmental capacity decreases the consumer population to the point where predation can serve as an additional control on the population, leading to a dramatic further decrease in the population. Once the consumer population is reduced to a minimal level, the forest can recover, leading to an increased environmental capacity, which eventually renders the predators ineffective in population control again. Delicate balances of the various processes are necessary to effect this cycling behavior, with other scenarios also possible. If the maximum predation level is above the range necessary for cycling, the consumer population can stabilize at a low level with the resource at a healthy level. Paradoxically, when the maximum predation is below the range for cycling, the consumer population also stabilizes at a low level, this time with the resource at a catastrophic level as well. The consumers are most successful in the case where the extent to which they injure the forest is sufficiently low ($\gamma < 1/4$). In this case, the drastic decrease in tree health is avoided and the consumer population can become endemic at breakout levels. Thus, natural selection pressure on the consumer, as well as that on the resource, acts in the direction of reduced impact of the consumer on the resource. This phenomenon helps explain why it is common for invasive species to be very damaging to an ecosystem—in the case of a sudden invasion, as compared to a gradual invasion resulting from natural changes in organism ranges, there is no time for selection pressure to act to stabilize the system.

REFERENCES

[1] Brauer, F. and C. Castillo-Chavez (2001). *Mathematical Models in Population Biology and Epidemiology*, Springer-Verlag, New York.
[2] Deng, B. (2001). Food chain chaos due to junction-fold point, *Chaos*, **11**: 514–525.
[3] Fenichel, N. (1979). Geometric singular perturbation theory for ordinary differential equations, *J. Diff. Eq.*, **31**: 53–98.
[4] Fowler, A.C. (1997). *Mathematical Models in the Applied Sciences*, Cambridge University Press, Cambridge.
[5] Holling, C.S. (1959). Some characteristics of simple types of predation and parasitism, *The Canadian Entomologist*, **91**: 385-389.
[6] Istas, J. (2005). *Mathematical Modeling for the Life Sciences*, Springer-Verlag, New York.
[7] Logan, J.D. (1997). *Applied Mathematics*, 2ed, John Wiley and Sons, New York.
[8] Ludwig, D., D.D. Jones, and C.S. Holling (1978). Qualitative analysis of insect outbreak systems: The spruce budworm and forest, *J. Animal Ecol.*, **47**: 315–332.
[9] Muratori, S. and S. Rinaldi (1992). Low- and high-frequency oscillations in three-dimensional food chain systems, *SIAM J. Appl. Math.*, **52**: 1688–1706.
[10] Rinaldi, S. and S. Muratori (1992). Slow-fast limit cycles in predator-prey models, *Ecol. Mod.*, **61**: 287–308.
[11] Segel, L., M. Slemrod (1989). The quasi-steady-state assumption: a case study in perturbation, *SIAM Review*, **31**: 446–477.

Received on March 30, 2006. Accepted on April 24, 2006.

E-mail address: gledder@math.unl.edu